Screening method for platform conductor integrity assessment for life extension prioritisation

SCREENING METHOD FOR PLATFORM CONDUCTOR INTEGRITY ASSESSMENT FOR LIFE EXTENSION PRIORITISATION

Ramesh Ramasamy [1*], Zainah Ibrahim[1], Hwa Kian Chai[2]

[1] Faculty of Engineering, University of Malaya, 50603 Kuala Lumpur, Malaysia.

[2] School of Engineering, University of Edinburgh, EH8 9YL United Kingdom

* Corresponding Author: ramasamy.ramesh@gmail.com; ramesh.ramasamy@siswa.um.edu.my

Abstract

Most of the major oilfields in the North Sea, Persian Gulf and South China Sea are becoming very mature, with their assets exceeding their calculated design life. ~~The severe corrosion~~Severe corrosions on the metallic structures of oil wells consisting of the conductor and casings, combined with spalling of annular cement forming the barriers can result in catastrophic events leading to structural collapse and wellhead vertically dropping onto the platform deck. With the collected inspection records, a systematic approach is deemed essential to assess the in-place condition of these wells and to categorise them for life extension works. This paper presents a simplified screening method for the structural integrity assessment of platform conductors towards the end of their design life and the prioritisation which follows thereafter for life extension operations by bridging the gap between design data and inspection records. The deterministic and probabilistic integrated approach is taken to address this problem, by considering the information collected from the as-built design records to the in-place inspections, coupled with the operating and metocean loads. The pragmatic and novel conductor operating guideline curves are proposed and constructed to present the evaluated integrity states, which will enable operators to rapidly categorise conductors for rehabilitation. ~~The~~This screening method is applied to a group of 40-year old water injection wells, and is demonstrated to have the practical prospect, and can be automated to provide a robust and effective assessment technique.

Keywords: Well Integrity; Platform Conductor; Cement Top-Up; Structural Reliability.

~~**Highlights:**~~

- ~~This paper is concerned with the problems facing operators of mature oil fields, looking into life extension of ageing offshore wells;~~
- ~~We propose a simplified and systematic method in undertaking ageing well conductor integrity assessment facing operators worldwide;~~

- ~~The method consists of deterministic and probabilistic analyses techniques to prioritise critical conductors for rehabilitation based on recommended practices and novel possibility considerations;~~
- ~~The gap between design data and inspection records are bridged to highlight and address the current integrity state;~~
- ~~The pragmatic repair prioritisation guideline curves are developed to enable rapid integrity screenings over vast mature fields;~~
- ~~A case study of 20 ageing well conductor samples from the Persian Gulf is used to illustrate the proposed workflow.~~

Formatted: Font: Bold

1. Introduction

Well integrity is perceived commonly as the actions leading towards reducing the risks of release of formation fluids into the environment during its operating lifespan. NORSOK [1] is a functional governing standard in matters concerning well integrity, and specifies the minimum requirement of a two-barrier well construction to prevent any leaks to the environment. The conductor and casings fall into the category of the well structural barrier, along with the annuli cement. Typical wells are designed for 25 years of service life, and operators worldwide are beginning to encounter wells operating beyond 30 years such as in the South China Sea (offshore Malaysia), and even up to 40 years, in some areas such as the North Sea [2] and the Persian Gulf. An example of a shallow water platform is shown in

Figure 1, highlighting the conductors, followed by the well construction layout inside the conductor, in Figure 2.

Figure 1: Shallow Water Jacket Platform in the Persian Gulf, Showing Typical Conductor Arrangement [4]

Continued services are usually expected ~~of~~from these older wells for several reasons. The primary reason is due to availability of significant amount of reserves remaining in the reservoir, accompanied by excessive ~~cost~~costs in replacement/abandonment activities. This is usually followed by requirement from the operator to maintain the existing platform whilst an alternative long-term solution is being developed, either the construction of a new platform, artificial islands [3] or tie back options. In any of these cases, the integrity of the wells must be kept pristine if extended service life is expected. It is common for operators to carry out scheduled site inspections and surveys to monitor the integrity of their wells, and it is very likely that these data are underused or misinterpreted in evaluating the integrity of ageing wells, potentially resulting in catastrophic failures such as casing collapse ~~and~~, or wellhead and surface tree settlement onto the platform deck.

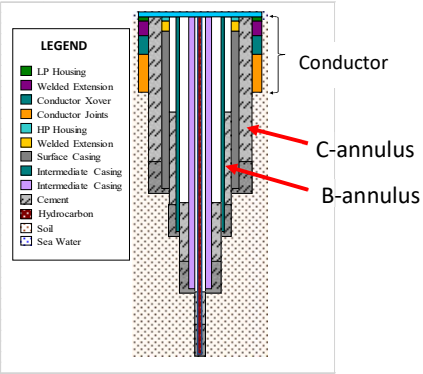

Figure 2: Platform Well Construction Schematics

In an ageing well, the heavy external corrosion on the conductor and ~~casing~~casing's outer diameter (OD) will result in the loss in overall stiffness to resist the topside weights and environmental loads. In areas with large pits and holes, seawater ingress will cause internal corrosion on the conductor inner diameter (ID), and to some extent the surface casing ID too. The continued conductor ID corrosion can result in rust flakes formation [4][5] which will in turn diminish the annular cement capacity to bond with the pipes inside the C-annulus effectively, and over time, will cause the cement shortfall, i.e. the cementation losing its shear bond capacity and dropping farther downhole [4][6]. These occurrences are depicted in Figure 3.

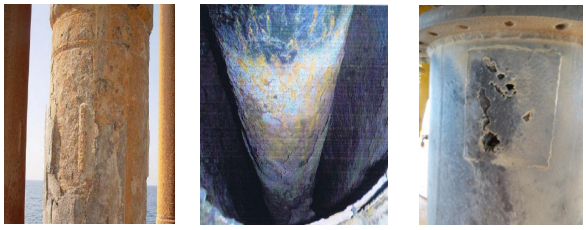

(a) (b) (c)

Figure 3: Site Inspection Showing (a) Conductor OD Corrosion, (b) Annulus Cement Shortfall, and (c) Severe Surface Pitting [4]

Under potentially high loading from the well topsides equipment (axial) and the environment (bending), and from the reduced stiffness ~~form~~from the ~~heavy~~severe wall loss and cement shortfall, possible collapse of the conductor/casing pipes can occur, resulting in the wellhead and tree to vertically drop down (vertical settlement) onto the platform decks [3][7], shown in Figure 4.

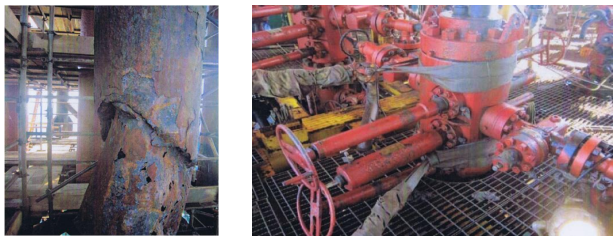

(a) (b)

Figure 4: Post Incident Inspection Showing (a) Collapsed Conductor Pipe and (b) Surface Tree Vertical Drop onto Deck [4]

2. Deterministic Methodology

2.1 Review of Inspection Data

The inspection records, consisting of ultrasonic (UT) based spot corrosion measurements consist of ~~circumferential~~ remaining wall thickness (WT) measurements on the conductor at specified elevations, around the circumference. More advanced methods are also available utilising the pulse eddy current (PEC) [7] or electromagnetic (EM) based system [8] which provides the mapped image of the wall profile in contoured colour scheme. A UT spot reading of a sample of 5 units of 40 years old conductors in the Persian Gulf with is shown in Figure 5 [8], indicating a typical magnitude of 60% wall loss at the splash zone region. The UT process is limited by its ability to measure remaining WT on reasonably good surface conditions, and presence of severe pitting and surface degradation specifically at the splash zone region (defined as ±2m from mean sea level, MSL) will present restrictions. Therefore, the same WT as measured at the top of the splash zone can be used throughout the splash zone. Visual inspections have shown that below the splash zone, in the subsea segments, the presence of marine growth can indirectly prevent further aqueous corrosion, and almost-nominal WT have been discovered upon surface cleaning [4][7][8].

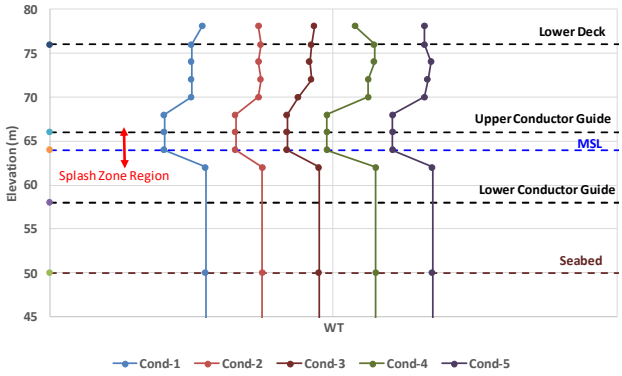

Figure 5: UT Spot WT Reading on 30in Conductors from the Same Field

Based on the measured WT on the conductor, a cross sectional assessment can be carried out for each elevation for the cross-sectional area (A) and its second moments (I_{xx}, I_{yy}), as follows:

$$A = \int \frac{1}{2}(R_i - r_i)\, d\theta$$

Equation 1

where R_i, r_i and θ are the outer radius, inner radius and the section angle between each UT reading respectively at elevation i.

$$I_{xx} = \int (y')^2\, dA_i \quad ; \quad I_{yy} = \int (x')^2\, dA_i$$

Equation 2

where y' and x' are the centroid distance to the x-axis and y-axis of each UT measurement section respectively.

Sectional properties can be evaluated using Equation 1 and Equation 2, for the corroded conductor pipe to be input into the global numerical model. A crude assumption that the axial loads are resisted by the average cross section, and the bending loads are resisted by the minimum cross section can also be used as a preliminary estimate, at local regions such as the splash zones, to conservatively assess the local stresses.

The annular cement elevations or top of cement (TOC) also provides crucial information on the overall well integrity, on the axial load mitigation in the event of any string collapse due to excessive corrosion, besides providing barriers between the hydrocarbon and the environment. ~~Inspections show,~~The inspections reveal that on average~~,~~ most well systems display absence of cement inside its C-annulus, i.e. between the 30in conductor and the 13-3/8in surface casing, as shown in Figure 6, accessed from the top of the conductor with a borescope device [6]. The B-

annulus will be unfeasible to access in majority cases, hence impossible to inspect without making a semi-destructive cut-out on the surface casing.

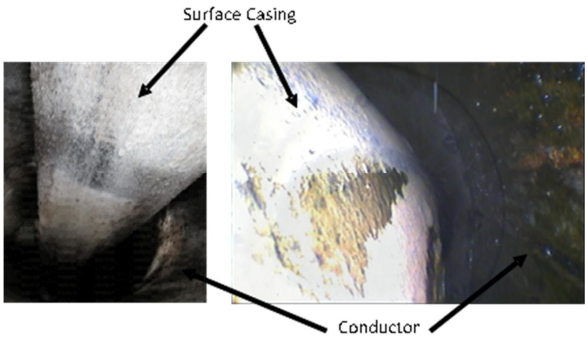

Figure 6: Borescope Inspection of the C-Annulus

Without any tangible quantification of the shortfall length, it will be impossible to assess the effect of the annulus cement, especially if the shortfall extends ~~for~~to hundreds of metres beneath the access point. It is therefore proposed that a range of shortfall combinations be considered to assess the entire spectrum of scenarios, from the best possible scenario (full cement) to the worst-case scenario (no cement), with some intermediate scenarios, as shown in Table 1. The intermediate points can be scalable to suit any water ~~depth~~depths and casing set ~~depth~~depths.

Table 1: Possible Cement Shortfall Scenario

Case	C-Annulus depth (or length) below wellhead, m	Case	B-Annulus depth (or length) below wellhead, m
C1	0[1]	**B1**	0[1]
C2	80	**B2**	80
C3	300	**B3**	300
C4	800	**B4**	800
C5	1700	**B5**	1700
C6	None[2]	**B6**	None[2]

Note:
1. Full cement inside annuli up to wellhead;
2. No cement inside annuli up to set depth of surface casing.

This will provide a combination of 36 scenarios for the probable cement situations in an ageing well and will provide a sensible estimate of the well integrity in the following sections of this paper.

2.2 Conductor Axial Preload

This section first discusses the calculation of the well axial preloads on the conductor, as ~~a~~the result of the well construction sequence. The axial preload is defined to be the effective weight acting at the wellhead, and supported by the conductor, which sums to the total axial load at the top of the conductor. The platform ~~well~~well's (Figure 2) drilling and installation are presented in Table 2 depicting the major activities for the conductor-casing-tubing string configuration, with the wellhead and surface tree at the beginning of the operating stage.

Table 2: Platform Well Major Construction Sequence

Stage	Activity	Duration (Days)
i	Drilling of 36in hole, installing the 30in conductor and cementing the outside annulus top the seabed.	3
ii	Drilling of 17in hole for 13-3/8in Surface casing and cementing of its outside annulus.	7
iii	Connecting spools and installing of the wellhead	1
iv	Running of BOP and installing on wellhead.	1
v	Drilling of 12in hole for 9-5/8in Inner casing and cementing of its outside annulus.	15
vi	Drilling of 5in hole for the 3-1/2in tubing, and installing packer downhole, with centralising cementing	7
vii	Removing BOP and Installing Surface Tree.	1

The casing strings [9] are represented as linearised axial springs with stiffness K_1, K_2, K_3 and K_4 for the 30in conductor, 13-3/8in surface casing, 9-5/8in inner casing and the 3-1/2in tubing respectively, where $K_1 = EA_1/L_{eff,1}$ and so on for each string of nominal cross sectional area A and the effective free length L_{eff}. All installed weights (W) are considered to be the buoyant weights in seawater for the conductor and cement/air for the internal strings supported at the top of the strings, depending on the fluid filling the respective annulus. This is shown in a free body diagram in Figure 7. The total axial preload at the top of the conductor can be evaluated at each well construction sequence depicted in Table 2, and are summarised in Table 3, for each corresponding stage.

Formatted: Font: Italic

Formatted: Font: Italic

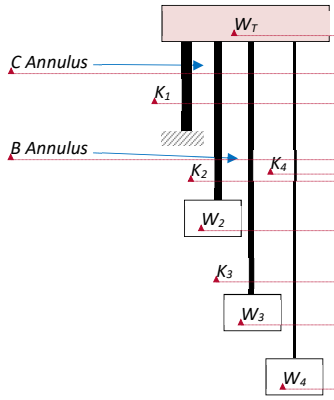

Figure 7: Platform Well Free Body Diagram

Table 3: Axial Preload Calculation

Stage	Total Added Top Weight, W	Available Total Stiffness, K	Axial Preload			
			F_1	F_2	F_3	F_4
i	0[a]	K_1	0	0	0	0
ii	W_2[b]	K_1	W_2	$-W_2$	0	0
iii	W_{wh}	$K_1 + K_2$	$F_{1,ii} + \frac{K_1}{K_1+K_2} W_{wh}$	$F_{2,ii} + \frac{K_2}{K_1+K_2} W_{wh}$	0	0
iv	W_{bop}	$K_1 + K_2$	$F_{1,iii} + \frac{K_1}{K_1+K_2} W_{bop}$	$F_{2,iii} + \frac{K_2}{K_1+K_2} W_{bop}$	0	0
v	W_3	$K_1 + K_2$	$F_{1,iv} + \frac{K_1}{K_1+K_2} W_3$	$F_{2,iv} + \frac{K_2}{K_1+K_2} W_3$	$-W_3$	0
vi	W_4	$K_1 + K_2 + K_3$	$F_{1,v} + \frac{K_1}{K_1+K_2+K_3} W_4$	$F_{2,v} + \frac{K_2}{K_1+K_2+K_3} W_4$	$F_{3,v} + \frac{K_3}{K_1+K_2+K_3} W_4$	$-W_4$
vii	$W_{tree} - W_{bop}$	$K_1 + K_2 + K_3 + K_4$	$F_{1,vi} + \frac{K_1(W_{tree}-W_{bop})}{K_1+K_2+K_3+K_4}$	$F_{2,vi} + \frac{K_2(W_{tree}-W_{bop})}{K_1+K_2+K_3+K_4}$	$F_{3,vi} + \frac{K_3(W_{tree}-W_{bop})}{K_1+K_2+K_3+K_4}$	$F_{4,vi} + \frac{K_4(W_{tree}-W_{bop})}{K_1+K_2+K_3+K_4}$

Notes:

a) *Conductor is set to be supported by the bottom soil bearing*
b) *As a conservative measure, the surface casing is supported by conductor to assess both the bottom soil bearing and the bottom connection*
c) *Well head is annotated by subscript 'wh';*
d) *Blowout Preventer is annotated by subscript 'bop';*
e) *Surface tree is annotated by subscript 'tree';*
f) *+(positive) represents compression, -(negative) represents tension;*
g) *The notation, F represents the preload on conductor, at stage i, and so on.*

The final conductor axial preload ($F_{1,vii}$) can then be summed to be as shown in Equation 3, and is compressive in nature, acting at the top of the conductor.

$$F_{1,vii} = W_2 + K_1\left[\frac{(W_{wh} + W_{bop} + W_3)}{K_1 + K_2} + \frac{W_4}{K_1 + K_2 + K_3} + \frac{(W_{tree} - W_{bop})}{K_1 + K_2 + K_3 + K_4}\right]$$

Equation 3

The unknown cement elevations, or top of cement (TOC) inside the C and B annuli between the strings is addressed by considering a range of scenarios of possible TOC, ranging from the most ideal scenario of full cement to the worst possible case of absolutely no cement in the annuli, with a few intermediate scenarios, i.e. TOC at mid-water depth or seabed, as well as the extreme possibilities shown in Table 1. Taking into account the buoyant installed weights (in seawater/cement) and the effective lengths of strings for each of these combination of TOC scenarios, a range of preload values can be calculated and the upper/lower bounds identified. The sum of the preloads on all strings at each stage must be equal to the total externally added weights of the topside equipment, thus ensuring equilibrium of the external and internal axial forces.

The injector wells typically have larger preload values than the producer wells. The effect of higher temperature in the producer wells relieves the compressive axial strain at the top of the well, thus reducing the preload. This results in additional concerns in ageing injector wells as compared to producer wells, despite the different risk classifications and failure consequences for both wells.

The considerable level of conservatisms built into this assessment method, although provides a potentially quick turnaround of screenings, but can be further reduced by detailed inspections of the corrosion and specialised inspection of the conductor preload itself. Executing the direct preload measurements [10] on the conductors can help streamline the well repair prioritisations to the absolute critical wells, thus optimising on cost and resources.

2.3 Annular Cement Assessment

The annular cement can be assessed in terms of its contribution to the overall well-conductor integrity and the alternative path provided for the axial loads in the event of downhole casing failure/collapse. The latter is shown schematically in Figure 8 (a) and (b) for a total cement shortfall scenario, where the occurrence of a downhole damage/collapse in the surface casing in (a) results in the axial load pushing the surface casing to move farther downhole, i.e. resulting in the wellhead dropping vertically down in (b). In the scenario of existing cement inside the annulus shown in (c) and (d), where the downhole casing damage in (c) results in the axial loads being mitigated through alternative path into the conductor, and possibly back into the casing farther away from the damage, or into the adjacent soil bearing.

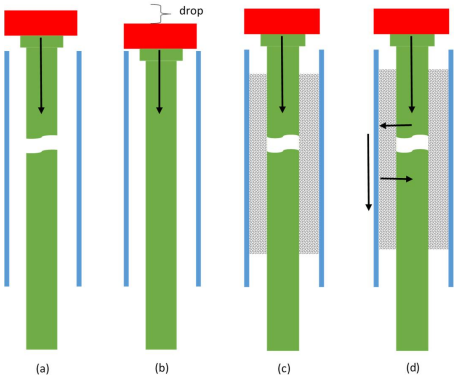

Figure 8 – Schematics Showing Contribution of Annular Cement to Post-Failure Behaviour, with (a) & (b) Downhole Casing Damage in Shortfall Zone, and (c) & (d) Alternative Load Path Provided by Cement

The annular cement effectiveness in providing a consolidation for the conductor and casing, depends very much on its bond strength with the metal surfaces. The bond strength is attributed to the combination of chemical reactions between the cement and metal, and the confinement pressure provided by the conductor which is translated into axial resistance of the total axial force acting on the string (F_{axial}) by the frictional coefficient on the casing OD along the length of the cement (L_{cem}). A characteristic bond strength (f_{buc}) estimate, empirically determined in [11] provides a conservative quantification in aged wells, with a safety factor under extreme event of 4.5 applied to account for any uncertainties, given as:

$$f_{buc} = \frac{1}{4.5}\left[\frac{9}{m}\left(\frac{t}{D}\right)C_L C_s\sqrt{f_{cu}} = \frac{F_{axial}}{\pi(OD).L_{cem}}\right]$$

Equation 4

~~Where~~where m, t, D and f_{cu} are the cement modular ratio to steel, thickness, diameter and compressive strengths respectively.

~~And~~and the coefficients C_L and C_S are the cement length to diameter ratio (taken as 0.7) and surface condition factor (taken as 0.5) respectively.

For a conventional Offshore Portland Cement (OPC), with nominal modulus of 30GPa and f_{cu} of 40MPa will produce a factored bond strength estimate of 0.1MPa inside the C-annulus. ~~For more~~The modern high strength cements [12]~~,~~ is able to provide a much higher characteristic bond of 0.9MPa or more, as well as providing ~~sound~~ reliability on good steel-cement bonds.

Another danger facing the surface casing specifically ~~in~~over a long cement shortfall is the exposed free span (un-cemented length) which has the tendency to buckle inside the

Formatted: Indent: First line: 0.52 cm

wellbore [13][14]. The casing coiling inside the wellbore forming a helical buckling will increase the bending moment at curvatures and combined with the contact forces at its interaction with the conductor, can potentially increase the downhole local stresses. This can lead to a possible downhole collapse, and also results in the wellhead vertically dropping down. For a shortfall length (*L*), and radial gap between conductor and surface casing (*r*), the pitch (*p*) caused by the helical buckling can result in a wellhead drop as shown in Equation 5.

$$Drop = L\left[\sqrt{\left(\frac{2\pi r}{p}\right)^2 + 1} - 1\right]$$

Equation 5

This phenomenon is observed more frequently in coiled tubing operations and is discussed in detail in [15], and empirical expression have been developed which can be used as a simple check to ensure all additional post-buckled stresses are within the acceptable limits.

2.4 Global Analysis

The environmental effects from the current and wave can be assessed numerically by constructing a global finite element (FE) model in ABAQUS [16], with a pipe-in-pipe assembly to represent the strings and the interactions between them and annuli cement or soil, and is schematically shown in Figure 9. The model consists of the conductor, surface casing and inner casing, modelled as two-dimensional pipe elements, with pipe-to-pipe contact spring elements exhibiting exponentially softened contact behaviour [16] to represent the radial gaps between them. This softened spring model will allow the inner casing to move inside the external casing/conductor within the available radial gap without any penetration beyond this gap. The pipe-soil interactions are modelled with the nonlinear soil *P-y* springs based on the geotechnical data, and the environmental currents and wave are modelled as distributed forces and Stokes' 5th Order wave theory respectively. The calculated preload is modelled as concentrated force acting at the top of the conductor, and the fixity applied at 50m below the seabed set as the model extent, which is sufficient to disperse any significant bending down to zero. Other boundary conditions such as the lateral ~~restrain~~restrains at the lower deck and supports provided by the platform guides are also modelled. The implicit dynamic solution sequence is executed to obtain the structural response to the applied loads and the resulting bending moment ~~distribution~~distributions can be extracted.

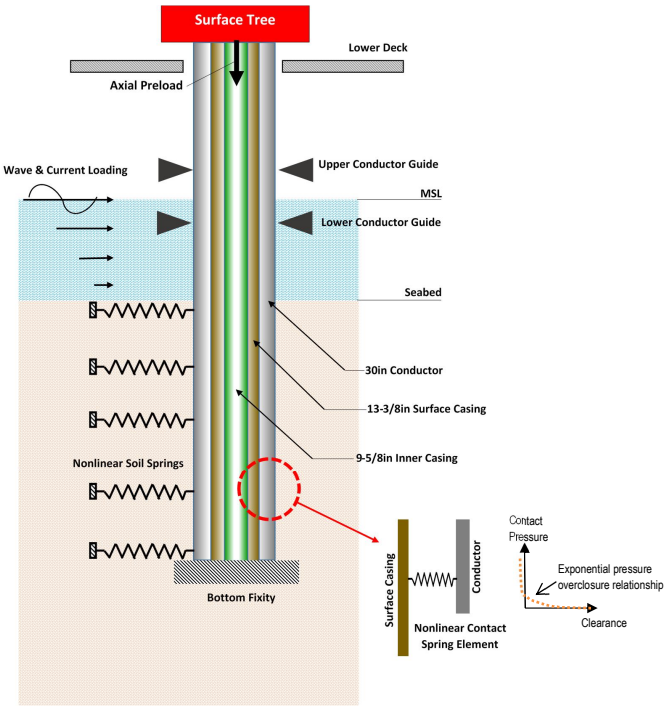

Figure 9 – Outline of Finite Element Model

The total absolute stress (σ_{total}) evaluations are carried out by adding the bending and axial stress components [17], derived from the absolute values of bending moment (M) and effective tension (axial preload, F_{30} + conductor weight up to the elevation, W) shown in Equation 6, and the resulting stresses are plotted in Figure 10.

$$\sigma_{total} = \frac{F_{30} + W}{A} + \frac{M_x\left({}^{OD}/_{2}\right)}{I}$$

Equation 6

The yield stress utilisation, or unity check (UC) is more convenient to check the exceedance of the specified minimum yield strength ($SMYS$) stipulated in API [9][17][18] such that $UC = \sigma_{total}/SMYS$. The standard allowable limits can be superimposed on the stress plots to visualise the exceedance magnitude and critical regimes, centred around the splash zone

region, which has maximum wall loss due to corrosion coupled with significant bending stresses, in addition to the axial preloads.

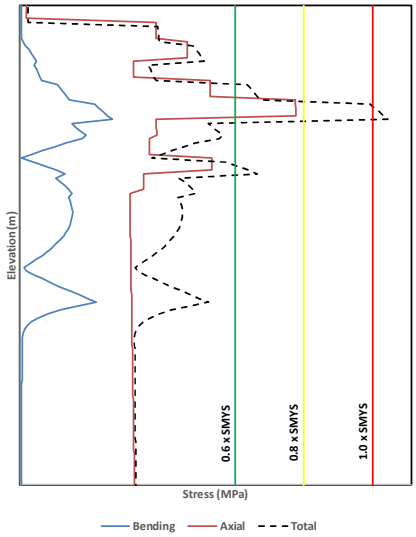

Figure 10 – Global Stresses on Corroded Conductor

2.5 Prioritisation Guideline

The global FE analyses are carried out for all the aged conductors which are being assessed for in-place integrity and life extensions, and it can be an arduous task to group the conductors according to their severity, thus a reliable and robust screening strategy is required to categorise these conductors. The consistent overstressing at the splash zone region due to the highest corrosion levels detected has resulted in the development of a screening technique focused at this elevation (± 2m from MSL) to easily prioritise for repairs. Typical routine inspections are carried out over a minimum of 4 equally-spaced circumferential points on the conductor, although the 8 to 16-points measurement or the full 360° scanning comes with greater accuracy with proportional cost implications. Therefore, this technique also must cater for the fact that any detailed inspections in the future to be carried out at this section, can be incorporated into this guideline for a more comprehensive evaluation.

The inspected remaining WT on the conductor at the splash zone can be divided into the minimum WT and the average WT. Since any number of point measurements carried out will converge towards a specific minimum and average WT (or OD, since OD = nominal ID + 2.

WT) value on the conductor, therefore the minimum/average WT based guideline is deemed adaptable regardless of any inspection technique employed, and is shown in Figure 11 for a range of minimum and average WT. So, each conductor deemed suitable for continued operation must comply to having a certain minimum WT, and associated average WT at the splash zone to ensure sufficient structural resistance is available to conform with the allowable stresses. For example, the minimum WT of 8mm, requires an average WT of 17.5mm to conservatively remain within the 0.6 operating allowable limit, or 10.4mm for the 0.8 extreme allowable limit.

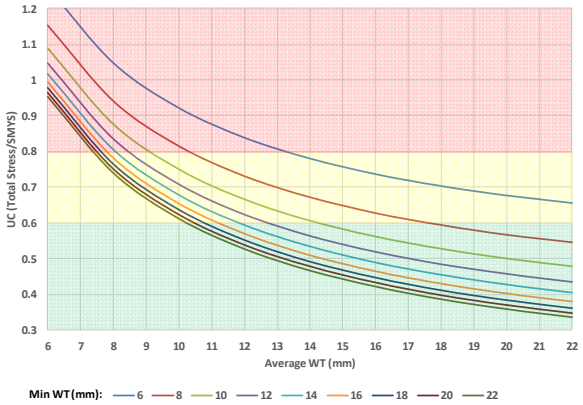

Figure 11 – Conductor Integrity Guideline Curve

This chart will provide the integrity team who is carrying out facility checks to confidently mark conductors based on their severity and their priority for repairs action, based on current inspections, as-built preloads and global analyses. However, certain levels of conservatisms are present in these steps leading to these guideline curves, particularly on the axial preload estimates. The unknown condition of the bottom soil bearing, cement bond conditions and actual degree of downhole corrosions have been taken into account by adequate safety factors and conservatively factored ~~resistive~~load capacities, thus a structural reliability analysis (SRA) will be implemented to rationalise the prioritisation of these conductors for life extension.

3. Probabilistic Framework

3.1 Assessment Accuracy and Uncertainties

The accuracy of the deterministic assessments presented in the preceding section of this paper depends on the following assumptions:

i. Well topside and inner string/tubing weights are supported primarily by the conductor (and in some cases with the surface casing), hence forming the basis for the axial preload calculations;
ii. The soil bearing is sufficient in resisting the conductor vertical movement, therefore providing vertical fixity;
iii. Corrosion measurements, although taken at fewer points around conductor circumference, are sufficient in mapping the minimum and average wall loss on the conductor;
iv. Remaining annular cement is assumed to provide adequate bond strength to the casing-conductor, within the applied safety factor limits;
v. Probabilistic consequences of the metocean conditions are ignored, as the main focus is on the Persian Gulf with very benign sea conditions.

To account for these uncertainties, and to quantify a failure probability to the conductors, the probabilistic framework will be setup to address these issues, and also to provide a statistical foundation to the assessment of the hundreds of well conductors within the same field based on the inspected sample wells.

The First Order Reliability Method (FORM) and the Monte Carlo Simulation (MCS) method are selected to be most practical for their implementation into the ageing conductor integrity assessments. Although computationally expensive, MCS can be an easy check to quickly assure the order of the obtained failure probabilities from FORM.

3.2 FORM

The uncertainties, randomness and non-trivial nature of the parameters involved in conductor integrity assessment (X), dictate the potential use of FORM to statistically evaluate the structural capacity and to ensure its exceedance over the operational demand. Successful applications of FORM in structural evaluations have been reported in [19] and [20]. The development of the nonlinear limit state function (LSF) (detailed in Section 3.4) labelled as $g(X)$, based on Equation 6, such that

$$g(X) = \textit{Maximum stress} - \textit{Allowable stress}$$

Equation 7

where maximum stress is calculated based on Equation 6, and the allowable limit is 0.6x*SMYS* [17] as a conservative limit.

Transforming the variables X into a standard normal space U, in terms of the mean (μ) and standard deviation (σ):

$$X = \{\sigma\}.\{U\} + \{\mu\}$$

Equation 8

Since the main parameters involved in the conductor integrity assessment (X_i, i=1,2,3…) have their associated mean (μ_i, i=1,2,3…) and standard deviations (σ_i, i=1,2,3…), the standard normal space variables can be written as:

Formatted: Font: Italic
Formatted: Font: Italic
Formatted: Font: Italic

$$X_1 = \sigma_1.U_1 + \mu_1\,;\; X_2 = \sigma_2.\,U_2 + \mu_2;\; X_3 = \sigma_3.\,U_3 + \mu_3;\; \ldots\ldots$$

or

$$U_1 = \frac{X_1-\mu_1}{\sigma_1};\; U_2 = \frac{X_2-\mu_2}{\sigma_2};\; U_3 = \frac{X_3-\mu_3}{\sigma_3};\; \ldots\ldots$$

Equation 9

for each parameter, and $g(X)$ will now have been converted into the normal space $g(U)$ as a function of U_1, U_2, U_3….such that:

$$g(U) = F(U_1,\, U_2,\, U_3,\ldots U_n) - F(U_{n+1}) = 0$$

Equation 10

The reliability index (β) is defined as the shortest line connecting the optimal solution to the LSF, as shown graphically in Figure 12, and can be evaluated by iterative technique for a nonlinear LSF at intrinsic design point U^*, such that $U^* = [u_1, u_2, u_3,\ldots u_n]$ and that the constraint $g(U) = 0$ is satisfied. The mathematical expression for β is as shown in Equation 11.

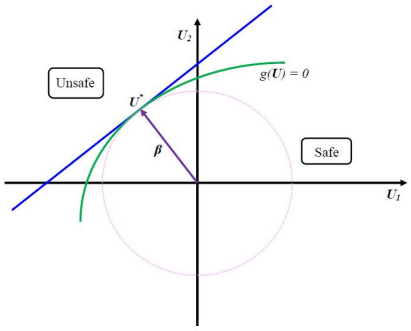

Figure 12: Graphical Representation of Reliability Index

$$\beta = -\frac{U^* G^{*T}}{\|G^*\|}$$

Equation 11

$$\text{where } G^* = \left\{\frac{\partial g(u)}{\partial u_i}\right\} \text{ and } \|G^*\| = \sqrt{\sum_{i=1}^{n}\left[\frac{\partial g(u)}{\partial u_i}\right]^2}$$

For non-normal distributed parameters, the Hasofer-Lind's reliability index method for more general case can be employed to compute the value of β, using the equivalent mean and equivalent standard deviation values at every iteration, followed by the Rackwitz-Fiessler algorithm in Equation 12 to find the corresponding β for the subsequent iterations of state variables.

$$u_{i+1} = \frac{[\nabla g(u_i)^T u_i - g(u_i)]\nabla g(u_i)}{|\nabla g(u_i)|^2}$$

Equation 12

3.3 MCS

A more systematic and computer-friendly algorithm is the MCS method [19], and is becoming ~~ever so~~more popular in recent years in the field of engineering SRA. This method requires the generation of sufficient samples to observe the converged failure probability of the system. Similar to the FORM, MCS also requires the prior knowledge of the statistical distribution of the parameters involved. MCS involves the random selection of points for larger sample sizes, and can be achieved by any random number generator algorithm such as Box and Muller transformations [22]. For a normalised LSF *g(U)* consisting of *N* sample points, rearranged such that *g(U)<0* for a safe operation, and an indicator I_g with a value of unity of the limit is satisfied, or nil otherwise, i.e. structural capacity exceeds the demand, the probability of failure can directly be evaluated from MCS as follows:

$$P_f = \frac{1}{N}\sum_{i=1}^{N}[I_g G(U_i)] < 0$$

Equation 13

The reliability index from the MCS (and FORM) can then be calculated from the inverse of the normalised failure probability distribution function, such that:

$$\beta = -\emptyset^{-1}(P_f)$$

Equation 14

3.4 Limit State Function (LSF) and Variables

For both the FORM and MCS framework, the determination of the LSF in the form of a global structural analysis can be carried out in an FE package for each conductor system, with the geometrical parameters, and loading applied as per the designated statistical distribution which will be discussed in the proceeding section of this paper. The outcome from the global FE will be fed into the response surface method (RSM) to generate a representative LSF by curve-fitting the meta-model with specific slopes (*a, b, c*…) which will be used in the Rackwitz-Fiessler algorithm in Equation 12. A nonlinear meta-model or RSM can take the form in Equation 15, which replaces the original LSF with (*2N+1*) unknowns and equal numbers of simultaneous equations for every

state variable X_i and X_j. This is a generic expression applicable for every conductor within the same field, within approximate water depths and similar environmental conditions.

$$R(x) = a + \sum_{i=1}^{N} b_i X_i + \sum_{j=1}^{N} c_i {X_j}^2$$

Equation 15

The limit state variables, in the case of the well-conductor structures, are ideally defined in terms of its geometrical and material properties, corrosion, loads and its allowable load capacities. The output from the deterministic FE global response will provide the equivalent stresses for the combination of variables with respect to their individual distribution functions.

The corrosion levels measured for a sample of 5 conductors along 10 elevation points, taken from the entire population of over 800 conductors across the field are handled by bootstrapping [23][24]. Bootstrapping belongs to the inferential statistics family, and involves drawing large number of pseudo-random repetitions of samples with replacements from the same population for large number of times. This is proven to be an effective method in gathering empirical or 'phantom' samples for any studies based on the original 'surrogate' samples. This technique is also based on the assumption that the distribution of the drawn sample is a good approximation to the distribution of the entire population.

In the case of the conductor corrosion measurements, as shown in Figure 5, the bootstrapping of the original data over 100, 1000 and 10000 times result in the normalised distribution for the minimum WT at splash zone, shown in Figure 13. This highlights the need for large number of phantom samples to obtain a reasonably good representation of the population.

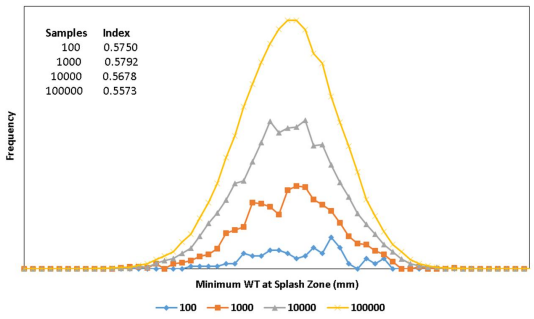

Figure 13: Normalised Histogram for Bootstrapping of Corroded Splash Zone WT

4. Case Study

A group of 20 platform conductors averaging about 40 years old ~~on~~installed over. injector wells with 90m set depth, located in a field of 15m water depth, and consisting of 30in (OD762mm x 405kg/m), 13-3/8in (OD340mm x 101kg/m), 9-5/8in (OD244mm x 70kg/m) and 3-1/2in (OD89mm x 13.7kg/m) strings are studied to illustrate the methods described earlier. The corresponding *SMYS* are 244MPa, 379MPa, 517MPa and 551MPa respectively. The combined weight of the wellhead and tree is approximately 5000kg. The UT spot measurements taken around the circumferences and along the elevations are used to obtain the minimum and average WT at splash zone region, and plotted in Figure 14 showing about 18% to 70% extreme wall losses, primarily at the splash zone regions.

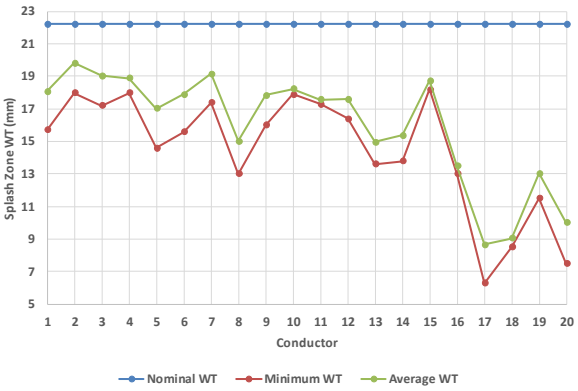

Figure 14: Inspected Splash Zone WT

The maximum surface current is 1.5m/s and the associated wave height is 8m with a period of 9s ~~in an~~under extreme storm ~~condition~~conditions, with calcarenite soil type reported up to 50m beneath seabed. The total depth of the well is approximately 3km below the seabed, with the surface casing extending to about 1.7km. Detailed inspections have revealed that all the conductors have cement up to the surface inside the B-annulus, and a range of shortfall from 0m to 1700m inside the C-annulus.

4.1 Deterministic Assessment

The preload calculations are carried out for a variety of C-annulus shortfall scenarios, for the range of B-annulus shortfalls (as per Table 1), and is plotted in Figure 15, with the lower and upper bound values of 3150kN and 4500kN respectively. The preload of 3600kN will be used to assess these wells as a most extreme case for a variety of C-annulus TOC from inspections (B-annulus TOC maintained at surface).

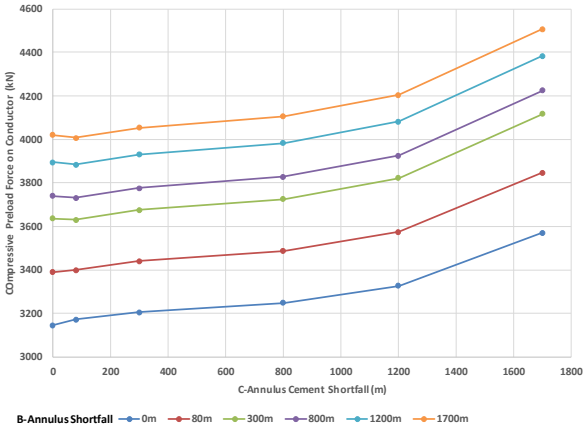

Figure 15: Calculated Conductor Axial Preload

The maximum bending moments and stresses at the splash zone is shown in Figure 16 for all the conductors based on global analyses. From the global analysis the extreme bending moment distributions can be obtained for the most severe conductor (Conductor-17, from Figure 14) with over 70% wall loss, and plotted in Figure 17 (a) with respect to the elevation showing an absolute maximum splash zone bending moment of about 260kNm, and 350kNm at the seabed. The corresponding stress utilisation is also plotted in (b) showing the overstressing at the splash zone region due to the ~~major~~severe wall loss, as predicted. Conductor 17, 18 and 20 shows exceedance of the extreme allowable limit (*UC* = 0.8), and therefore can be prioritised for repairs, unless detailed inspections carried out shows better average WT remaining around these conductors.

The maximum un-cemented free span length of the surface casing inside the C-annulus, at its full set depth of 1700m is checked ~~fort~~for any helical buckling inside the wellbore as proposed in [15], for the surface casing eccentricity of 50mm inside the conductor pipe, and an arbitrary casing topside force of 2000kN. ~~A~~The uniform corrosion of 20% of the nominal WT is also assumed throughout the length, since no reliable data for the surface casing can be obtained from the inspection. An estimate of the minimum length required to undergo helical coiling inside the wellbore is estimated at 185m, with maximum wellhead drop of 60mm and the additional bending stress of 66MPa due to the coil formations for the worst-case scenario. This will result in the UC of 0.7 when combined with the axial stress on the corroded surface casing, therefore presenting no immediate concern.

These deterministic assessments are very conservative and accounts for the uncertainties in the inspection process and the obtained design data, and the reliability aspect of these assessment can now be undertaken to quantify the failure probabilities.

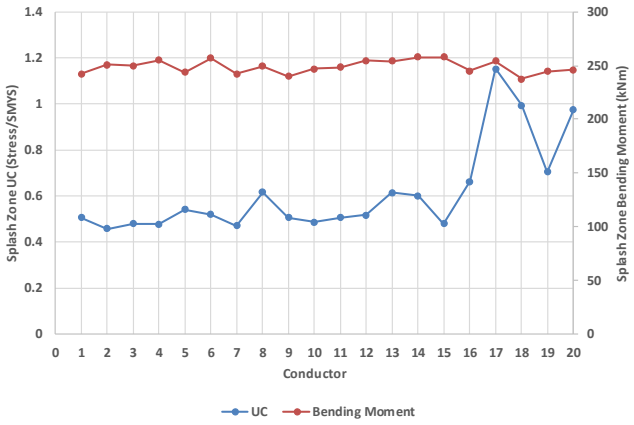

Figure 16: Bending Distribution and Resulting *UC* at Splash Zone on All Conductors

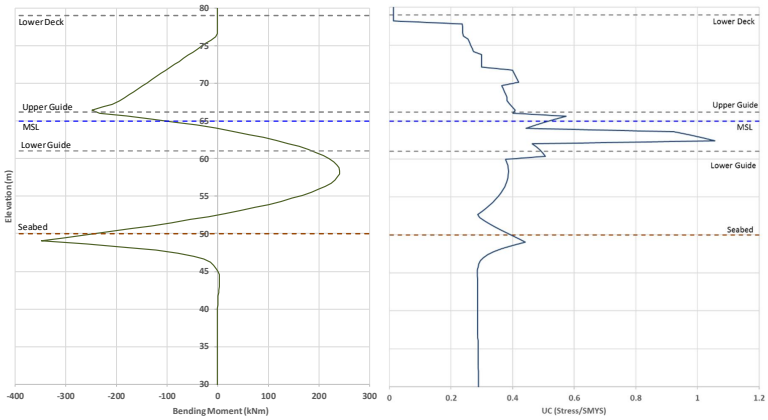

(a) (b)

Figure 17: (a) Extreme Bending Moment Distribution, and (b) Corresponding Stresses on Conductor-17

4.2 Probabilistic Assessment

The probabilistic well data, as be generated and summarised in Table 4 based on the inspections carried out on the 20 selected conductors consisting of the mean (μ) and standard deviation (σ) for the parameters of interest.

Formatted: Font: Italic

Formatted: Font: Italic

Table 4: Probabilistic Well Data

Parameters	Limit State Variable	Normal Space Variable	Statistical Distribution	μ	CoV
SMYS (MPa)	X_1	U_1	Normal	244	0.1
Conductor Preload Force (kN)	Deterministic Value Used				
Maximum SZ Bending (kNm)					
Minimum Splash Zone OD (m)	X_2	U_2	Normal	14.5	0.3
Average Splash Zone OD (m)	X_3	U_3	Normal	16.0	0.2

Note:

a) CoV is coefficient of variation, defined as ratio of standard deviation and mean, σ/μ.

b) $OD_{min} = ID_{nominal} + 2.WT_{min}$

c) $OD_{avg} = ID_{nominal} + 2.WT_{avg}$

First, the FORM is carried out by evaluating the limit state function (LSF) *R(x)* for the load demand and structural capacity parts accordingly at the splash zone region, such that *R(X) = Capacity – Demand ≥ 0* to ensure the survival. Various checks were carried out to study the contributions of the various parameters, and the minimum OD (X_2) and average OD (X_3) at the splash zone region are deemed the most influencing factor within acceptable limits. The Capacity and Demand terms are normalised to the allowable extreme limits (0.8 x *SMYS*) in this formulation, and the resulting regressed line fitting is shown in Table 5, and the residual plot comparing the predicted and numerically evaluated *UC* value in Figure 18. A nonlinear function is fitted into the system to best represent the behaviour with a 99% accuracy. The response surface method (RSM) can now be implemented to determine the failure probability (P_f) based on the derived LSF. The iterative steps taken to evaluate the reliability index, β is shown in Table 6 based on Equation 8 to Equation 12, and numerically converges to 1.520 after the 49th iteration for the developed complex LSF. This results in a failure probability of about 12.57%, or a reliability of 87.43% based on the 20 sample conductors with the simplified FORM assessments as shown.

Table 5: LSF for Conductor Maximum Stresses at Splash Zone Region

LSF	$R(X) = Capacity - Demand$ $Capacity = a_1X_1$ $Demand = a_2+a_3.X_2+a_4.X_3+a_5.X_2^2+a_6.X_3^2+a_7.X_2.X_3$
a_1	0.800
a_2	-583.636
a_3	917.5713
a_4	622.8583
a_5	-266.989
a_6	-68.3962
a_7	-680.487

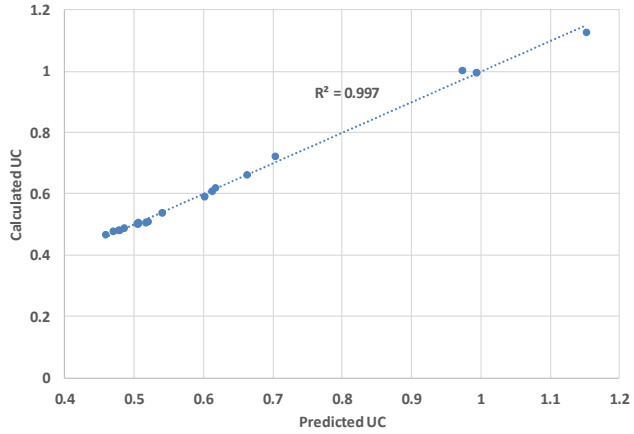

Figure 18: Residual Plot Showing Comparison Between the UC from Line Fit and Numerical Evaluations

Table 6: FORM-RSM Iterations Showing Evaluation of Reliability Index

Iteration	0	1	.....	49	50	51
β	0.000[a]	2.774		1.519	1.520	1.520
U_1	0.000[a]	-2.350		1.209	1.209	1.209
U_2	0.000[a]	-1.474		-0.921	-0.921	-0.921
$G(U)$	-2.09E+05	-5.06E+04	.....	-2.45E+05	-2.45E+05	-2.45E+05
$G^*(U_1)$	-6.38E+04	3.48E+04		6.42E+04	6.42E+04	6.42E+04
$G^*(U_2)$	-4.00E+04	-1.73E+04		-4.89E+04	-4.89E+04	-4.89E+04
$\|\|G^*\|\|$	7.53E+04	3.89E+04		8.07E+04	8.07E+04	8.07E+04
P_f[b]	39.89%	0.85%		12.58%	12.57%	12.57%

Note:
a) Initial estimate of the values set at zero;
b) Assumed standard normal distribution.

The Monte Carlo simulation (MCS) technique with the bootstrapped corrosion data is carried out to validate the failure probability obtained from FORM for the 20 samples. The generic API stress equation (Equation 6) are used to check the validity of the failure probability magnitude for a sample size of 100 to 1000000, and the results are presented in Table 7, for bootstrapped minimum/average OD's and normalised distribution for the other parameters. The failure probability converges towards 14.8% at 100000 sample sizes, and is within acceptable magnitude with the FORM-RSM evaluations.

Table 7: Failure Probabilities Obtained from MCS

Samples Size	P_f
100	22.00%
1,000	15.30%
10,000	14.62%
100,000	14.79%
1,000,000	14.76%

The SRA in the form of FORM and MCS evaluated this section, now lays the foundation for the risk assessments [25] to be carried out for the sample size (N), with each probability of failure (P_i) known, and the associated consequences of that failure (C_i), as shown in Equation 16. This can be further expanded to include a more comprehensive assessment of probabilities of the individual hazard (H) and the corresponding failures (F) and non-failures ($\overline{F}$). The subsequent categorisation of the well within the company predefined risk matrix can then be executed, as shown in Figure 19 to create planning for the rehabilitation of these wells.

$$Risk = \sum_{i}^{N} P_i . C_i = P(H).\{P(F|H) + P\left(\overline{F}\middle|H\right)\}.C(F)$$

Equation 16

		Consequences				
		Moderate	Serious	Major	Catastrophic	Disastrous
		1	2	3	4	5
Likelihood	5					
	4			X		
	3					
	2					
	1					

Figure 19: Example Risk Matrix for the Case Study

5. Conclusion

This paper has outlined a simplified method to undertake well conductor integrity evaluations towards life extension operations for continued service, as summarised in Figure 20, highlighting the major steps taken.

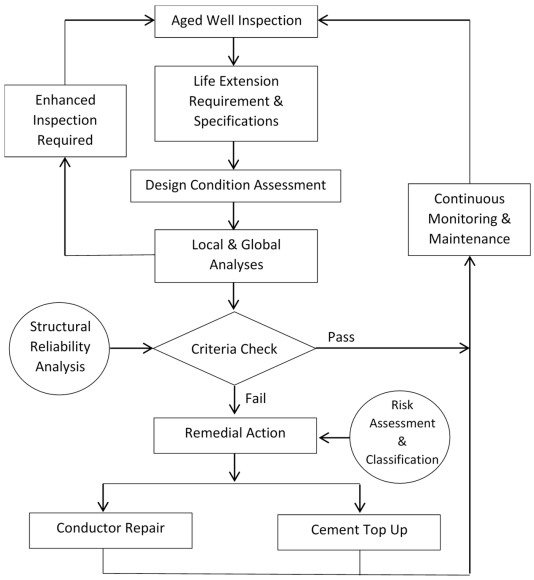

Figure 20: Well Conductor Simplified Integrity Assessment General Workflow

The deterministic method, based on global modelling in FEA considers the design data, where conductor preloads are evaluated to represent the residual loads carried forward from the as-built state of the well. The global analysis output will provide crucial information on requirement for any follow-on detailed inspections. The standard API recommended allowable criteria are used in determining the conductors which are fit-for-service and preliminary categorisation can be carried out for remedial works. The probabilistic based SRA will complement the deterministic analyses with the limit state based quantifications of failure probabilities in the entire population of wells within the field and the development of the risk classification matrix for life extension planning and scheduling of the critical wells.

The computational Monte-Carlo technique is also carried out with bootstrapped corrosion data (converted into conductor OD) to embody the entire population of well within the mature field This forms the systematic but simplistic assessment procedure for shallow water platform conductors, and can be undertaken by operators of mature fields within acceptable levels of conservatisms, as a first step towards life extension of ageing wells. This method also bridges the gap between the design data, inspection of in-place conditions to the integrity state of the wells, therefore enabling the integrity teams to prioritise wells accordingly. Although the actual remedial activities of the ageing wells are not within the scope of this paper, but standard repairs using clamps and sleeves for the conductors, and annuli cement top up to consolidate the surface casings have been successfully implemented as presented in [4][6][12].

Improvements and rationalisation of this simplified method is underway to incorporate detailed preload inspection techniques to provide accurate preload values on the conductors and surface casing, to better appraise the well prioritisations. Ultrasonic and other surface wave based non-destructive techniques (NDT) [10][26] are currently being studied for their practicality and applications into the offshore sector. This has the great potential of significantly optimising the outcome which will be reflected by the drastic cost savings for operators.

6. Acknowledgement

The authors wish to express their gratitude and appreciation to the academic support from the University of Malaya, Malaysia.

7. References

[1] NORSOK – "Well Integrity in Drilling and Well Operations". NORSOK-D010, Revision 3, August 2004.
[2] SHELL – "2011 Annual Environmental Statement For Shell U.K. Upstream Operations", 2011, www.shell.co.uk.
[3] Balmer, B. (2012). ADMA OPCO Development of Asset Replacement Plans for 20 Years for Zakum, Umm Shaif and Das Island. Society of Petroleum Engineers. doi:10.2118/161249-MS
[4] Ramasamy, R., AlJaberi, M., AlJunaibi, H. 2014. Ageing Offshore Well Structural Integrity Modelling, Assessment and Rehabilitation. ADIPEC, November 2014, SPE-171741-MS.
[5] S. Talabani, B. Atlas, M.B Al-Khatiri, M.R. Islam, An Alternate Approach to Downhole Corrosion Mitigation, J. Petroleum Science and Engineering, 26 (2000), 41–48.
[6] Husby, O. (2014, June). Draugen Surface Casing Corrosion. Speech presented at Shell Norske Well Integrity Seminar in Norway, Retrieved from https://www.norskoljeoggass.no.
[7] Munns, I., & Crouzen, P. (2007, November 5). Inspection of Offshore Platform - Well Surface Casings and Conductors. Lecture presented at SPE Applied Technology Workshop Well Integrity, Barcelona.
[8] Abdalla, D., & Fahim, M. (2013). Casing corrosion measurement to extend asset life. Oilfield Review, 3, 25.
[9] API – "Specifications for Casings and Tubings". API-SPEC-5CT, 8th Edition, July 2005.
[10] Ramasamy, R., Ibrahim, Z., Suhatril, M. Criticality of Conductor/Casing Integrity for Ageing Offshore Well Life Extension, Regional Marine and Mechanical Engineering Conference (ReMME), Malaysia, October 2016, Paper-16.
[11] U.K Department of Energy - "Grouted and Mechanical Strengthening and Repair of Tubular Steel Offshore Structures". UK Department of Energy, Offshore Technology Report OTH 88 283.
[12] Densit. (2016). Ducorit Ultra High Performance Cement [Brochure]. Denmark.
[13] B. Stahl, M.P. Baur, Design Methodology for Offshore Platform Conductors, Offshore Technology Conference, 5/5/1980, Houston, Texas, 1980, OTC-3902-MS.
[14] Timoshenko, S. P., and Goodier, J. N. (1970). Theory of Elasticity, 3rd Ed., McGraw-Hill, New York.
[15] Jiang Wu, H.C. Juvkam-Wold, Coiled Tubing Buckling Implications and Completing Horizontal Wells, SPE Drilling and Completions, March 1995, SPE-26336-PA.
[16] Abaqus Theory Manual version 6.11; 2011.
[17] API – "Recommended Practice for Planning, Designing and Constructing Fixed Offshore Platforms". API-RP-2A WSD, 21st Edition, December 2000.
[18] API – "Recommended Practice for Design of Risers for Floating Production Systems and TLPs". API-RP-2RD, 1st Edition; June 1998.
[19] Verderaime, V. (1994) "Illustrated Structural Application of Universal First-Order Reliability Method", NASA Technical Paper 3501, Retrieved from http://ntrs.nasa.gov.
[20] Cizelj, L.; Mavko, B.; Riesch-Oppermann, H. (1994) "Application of first and second order reliability methods in the safety assessment of cracked steam generator tubing", Nuclear Engineering and Design, 147.

[21] Metropolis, N.; Ulam, S. (1949). "The Monte Carlo Method". Journal of the American Statistical Association. American Statistical Association. 44 (247): 335–341
[22] G. E. P. Box and Mervin E. Muller, A Note on the Generation of Random Normal Deviates, The Annals of Mathematical Statistics (1958), Vol. 29, No. 2 pp. 610–611.
[23] Efron, B. *(1979). "Bootstrap methods: Another look at the jackknife".* The Annals of Statistics *7 (1): 1–26.*
[24] Davison A.C. and Hinkley D.V. (1997). Bootstrap Methods and their Application. Cambridge University Press, Cambridge.
[25] The International Organization for Standardization (ISO)– Petroleum and natural gas industries – "Offshore Production Installations – Guidelines On Tools and Techniques For Hazard Identification And Risk Assessment". ISO-17776, 1st Edition, 2000.
[26] R. Ramasamy, Z. Ibrahim, H.K Chai, T.F Chau, "Measurement of platform conductor preload in streamlining the life extensions of ageing offshore wells", Applied Ocean Research, Volume 65, April 2017, Pages 12-22, ISSN 0141-1187, http://doi.org/10.1016/j.apor.2017.03.004.